The effect of surfactant on the transient motion of Newtonian drops

W. J. Milliken
Chevron Oil Field Research Company, P.O. Box 446, La Habra, California 90633

H. A. Stone
Division of Applied Sciences, Harvard University, Cambridge, Massachusetts 02138

L. G. Leal
Department of Chemical and Nuclear Engineering, University of California, Santa Barbara, California 93106

(Received 24 June 1992; accepted 15 September 1992)

The effect of dilute, insoluble surfactant on the deformation and breakup of a viscous drop is examined. Two cases are considered: the deformation and stretching of a drop in a uniaxial extensional flow and the surface-tension-driven motion of an elongated drop in a quiescent fluid. Aside from rescaling the mean capillary force through an average decrease in the interfacial tension, surfactants alter the motion of a viscous drop through gradients in interfacial tension. The effects of surfactants are found to be most pronounced for small viscosity ratios, where Marangoni stresses substantially retard the interfacial velocity and cause the drop to behave as though it were more viscous. Surfactants are found to facilitate the formation of pointed ends during drop stretching, and this may explain the observation of tip streaming in experiments with viscoelastic drops. Surfactant gradients also allow drops to be elongated to a larger degree without producing end pinching.

I. INTRODUCTION

There are many important examples where the presence of surfactant critically alters the motion of immiscible fluids. Probably the best known is the effect of surfactant on buoyancy-driven motions of small bubbles. Except in very clean systems, the velocity of a rising bubble is substantially less than the classic Hadamard–Rybczynski prediction. In this instance, the surfactant is convected toward the rear stagnation point on the bubble surface, and the resulting gradient in interfacial tension retards the surface velocity and thus slows the bubble motion.

In this paper, we consider the influence of surfactant on the deformation and breakup of drops in extensional flow. The deformation of viscous drops in shear and extensional flows has received a great deal of attention in the literature dating to the pioneering work of Taylor.[1,2] A summary of the literature through 1984 can be found in the review paper by Rallison,[3] and more recent work is discussed by Stone.[4] However, in spite of the fact that surfactants are extremely common in practical applications, their influence on the deformation of a viscous drop is largely unexplored. Flumerfelt[5] has examined the effects of dynamic interfacial properties (interfacial viscosity and elasticity) on drop deformation and Greenspan[6,7] has examined the effects of surfactant on the deformation of a nearly spherical fluid drop. More recently, Zinemanas and Nir[8] numerically investigated the role of surface active elements in cell cleavage. However, to our knowledge, only Stone and Leal[9] have examined the effects of surfactant that arise solely due to its influence on the interfacial tension.

Stone and Leal,[9] hereafter referred to as I, studied the effects of insoluble surfactant on the *steady* deformation of a drop in a steady flow when that drop has the same viscosity as the suspending liquid. They determined that the degree of deformation is influenced by two phenomena: accumulation of surfactant at the ends of the drop and dilution of the overall surfactant concentration owing to drop deformation. The external flow (in this case, uniaxial extension) causes surfactant to be convected toward the ends of the drop, where it accumulates. Dilution of surfactant occurs because, as the drop deforms, its interfacial area increases, while the total amount of surfactant remains constant.

In this work we generalize I and consider a range of drop fluid viscosities, time-dependent drop motions, and a nonlinear equation of state for the interfacial tension. In a future publication we will address surfactant solubility. The problem and solution technique has been formulated in detail in I. Thus, in the next section, we only briefly outline the governing equations and the relevant dimensionless parameters. The interface deformation problem is solved using the boundary integral technique, while the convective–diffusion equation for the surfactant distribution is solved by a finite difference scheme. This approach is very efficient for our purposes, viz., to determine the motion of the interface. In Sec. III we present our results; a summary is given in Sec. IV.

II. PROBLEM STATEMENT

As shown in Fig. 1, a neutrally buoyant drop is suspended in an immiscible fluid of infinite extent with a fixed amount of insoluble surfactant adsorbed on the interface between the two fluids. Insoluble surfactant is, by definition, surfactant that is confined to the interface; the surfactant is not soluble in either of the fluid phases. Experimentally, this limit is approximated at low concentrations of surfactant when the partition coefficient strongly favors

 0899-8213/93/010069-11$06.00

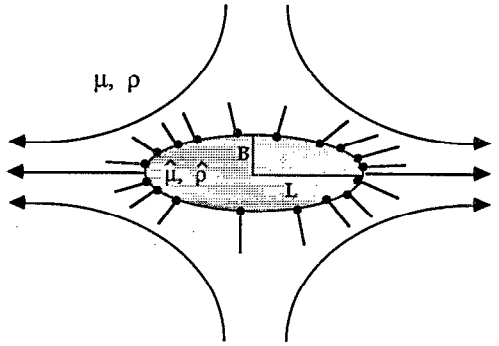

FIG. 1. A sketch of the problem. Not drawn to scale.

adsorption on the interface. The drop has a viscosity $\hat{\mu}$, the surrounding fluid has a viscosity μ, that is, in general, different, and λ denotes the viscosity ratio $\lambda=\hat{\mu}/\mu$. The interface between the fluids is characterized by an interfacial tension, σ, that depends on the local surfactant concentration.

We consider two problems. In the first, we examine the steady deformation and the unsteady stretching (breakup) of a drop in a steady, uniaxial, extensional flow. In the second, we investigate the interfacial-tension-driven motion of an elongated drop suspended in a fluid that is otherwise quiescent. The Reynolds number for both problems is much less than unity. The distribution of the adsorbed surfactant is determined by the competing effects of surface convection and diffusion.

The relationship between the interfacial tension and the local surface excess concentration of surfactant is referred to as the equation of state for the interfacial tension. For dilute surfactant concentrations, the equation of state is linear,

$$\sigma=\sigma_s(1-\beta\Gamma)=\sigma^*\left(\frac{1-\beta\Gamma}{1-\beta}\right) \tag{1}$$

and

$$\beta=\frac{\Gamma_0 RT}{\sigma_s}, \tag{2}$$

where σ is the actual interfacial tension, σ_s is the interfacial tension for a "clean" (i.e., surfactant-free) interface, Γ is the dimensionless surfactant concentration, $\Gamma\equiv\Gamma^*/\Gamma_0$, Γ^* is the surfactant concentration in moles per unit area, and Γ_0 is the reference surfactant concentration chosen here to be the initial uniform concentration of surfactant on the undeformed drop. The parameter β varies between zero (no surfactant effect) and unity; in Eq. (2), R is the gas constant and T is the absolute temperature. The magnitude of the interfacial tension for uniformly distributed surfactant at the equilibrium concentration, Γ_0, is $\sigma^*=\sigma_s(1-\beta)$.

Equation (1) was used exclusively in I and is a valid approximation for insoluble surfactant. Nevertheless, in this study, we also examine the importance of the equation of state. There are a large number of nonlinear equations available in the literature. We choose to consider

$$\sigma=\sigma_s\{1+\beta\Gamma_\infty[\ln(1-y)-(1/2)ky^2]\}, \tag{3}$$

where $y\equiv\Gamma/\Gamma_\infty$, Γ_∞ is the maximum (dimensionless) concentration for complete surface coverage as a unimolecular film, and k is a material parameter. When adsorption is described by a Frumkin adsorption isotherm and the surfactant solution is considered ideal, the interfacial tension can be written explicitly as Eq. (3).[10] Although, this equation is strictly valid only when the adsorption is described by a Frumkin isotherm, we use it here as an example of a typical nonlinear equation of state. For the parameter k, we use $k=2.52$, which was measured by Lin[10] for the surfactant Triton X-100. Note that in the linear limit of large Γ_∞, Eq. (1) is recovered, but that Eq. (3) diverges from Eq. (1), especially as Γ approaches Γ_∞.

The governing equations for the fluid mechanics and the surfactant mass transfer problems are presented below. For the deformation of a drop in uniaxial extension, it is convenient to nondimensionalize the equations with respect to the drop radius, a, the characteristic velocity scale σ_s/μ, and the characteristic time scale $\mu a/\sigma_s$. Although one could alternatively choose Ga as the characteristic velocity scale and G^{-1} as the characteristic time scale (where G is the magnitude of the undisturbed velocity gradient), the choice made here is convenient because it allows a single formulation both for the drop in a flow and the surface-tension-driven motion of the drop in a quiescent fluid.

The fluid motion is governed by the usual continuity and low Reynolds number momentum equations (Stokes equations) both inside and outside the drop,

$$\nabla^2\mathbf{u}=\nabla p, \quad \nabla\cdot\mathbf{u}=0, \tag{4}$$

and

$$\nabla^2\hat{\mathbf{u}}=\nabla\hat{p}, \quad \nabla\cdot\hat{\mathbf{u}}=0, \tag{5}$$

where $\mathbf{u}$ is the velocity, p is the pressure, and the overcaret refers to quantities inside the drop.

At the interface between the two phases we require continuity of the velocity and stress,

$$\mathbf{u}=\hat{\mathbf{u}}, \quad \mathbf{x}\in S, \tag{6}$$

$$\mathbf{n}\cdot\mathbf{T}-\lambda\mathbf{n}\cdot\hat{\mathbf{T}}=\left(\frac{\sigma}{\sigma_s}\right)\mathbf{n}(\nabla_s\cdot\mathbf{n})-\nabla_s\left(\frac{\sigma}{\sigma_s}\right). \tag{7}$$

Here $\mathbf{T}$ is the stress tensor, S denotes the fluid–fluid interface, ∇_s is the surface gradient operator $[\nabla_s=(\mathbf{I}-\mathbf{nn})\cdot\nabla]$, $\nabla_s\cdot\mathbf{n}$ is the local mean curvature, and $\mathbf{n}$ is the outward pointing unit normal. The function σ/σ_s is given by either Eq. (2) or (3). The kinematic boundary condition is written as

$$\frac{d\mathbf{x}}{dt}=(\mathbf{u}\cdot\mathbf{n})\mathbf{n}, \quad \mathbf{x}\in S. \tag{8}$$

Finally, far from the drop, the velocity must approach the free-stream velocity, which, for a drop in a steady uniaxial extension, is

$$\mathbf{u}\to\mathbf{u}_\infty(\mathbf{x})=C\begin{bmatrix}-\frac{1}{2} & 0 & 0\\ 0 & -\frac{1}{2} & 0\\ 0 & 0 & 1\end{bmatrix}\cdot\mathbf{x},\quad |\mathbf{x}|\to\infty, \tag{9}$$

where C is the capillary number $aG\mu/\sigma_s$. For the interfacial-tension-driven motion of an elongated drop in a quiescent fluid the far field condition is $\mathbf{u}\to 0$. Clearly this can be considered as the limit $C=0$.

Finally, the surfactant concentration on the interface is governed by the time-dependent surface convective–diffusion equation,[11–13] which can be written in dimensionless form as

$$\frac{\partial\Gamma}{\partial t}+\nabla_s\cdot(\Gamma\mathbf{u}_s)=\frac{1}{\gamma}\nabla_s^2\Gamma-\Gamma(\nabla_s\cdot\mathbf{n})(\mathbf{u}\cdot\mathbf{n})+j_n. \tag{10}$$

Here, $\mathbf{u}_s$ is the surface tangential velocity, j_n is the net flux of material to the interface (taken here to be zero), and γ is the parameter

$$\gamma=\frac{\sigma_s a}{\mu D_s}. \tag{11}$$

This parameter depends only on the material properties of the fluids. It can be interpreted as the ratio of the surface Péclet number, $\mathrm{Pe}_s=Ga^2/D_s$, to the capillary number, i.e.,

$$\gamma=\mathrm{Pe}_s/C. \tag{12}$$

In steady flows, we measure the deformation, D_f (Fig. 1), as a function of the capillary number, C, for fixed values of γ and β.

The numerical formulation and solution of this problem is also described in detail in I. The motion of the drop interface is determined by the boundary integral technique. The technique has found widespread use in the study of the dynamics of free boundary problems (see, for example, Refs. 14 and 15).

The mass transfer of surfactant on the interface is described by Eq. (10). We employ a finite difference formulation assuming quadratic variation in the concentration between collocation points. For economy, the mass transfer problem is solved at the same node points as are used for the interface representation in the boundary integral formulation. An implicit Euler scheme is used to advance the concentration distribution forward in time.

Twenty collocation points and a time step of 0.05 are used to determine the steady drop shapes (since we assume fore–aft symmetry, this amounts to 39 points describing the axisymmetric drop). As the drops stretch and become elongated, the number of collocation points is increased from 20 to 40. This number is further increased to 90 for the highly elongated shapes encountered in the capillary wave simulations. We are confident that this is a sufficient number of collocation points and a sufficiently small time step as our results show no observable changes in shape when either the number of points is increased or the time step decreased. The drop shape was considered steady when the normal velocity at all points on the interface was less than 0.0003. For small deformations of the drop from sphericity (small capillary numbers), an asymptotic prediction for the drop shape has been derived. It is available in the appendix of I. This asymptotic calculation is used to check the initial small deformation results obtained from the numerical procedure.

III. RESULTS

We present our results in three sections. In the first section, we consider steady drop shapes and assess the role of viscosity ratio on drop deformation. The majority of our results are contained in the second section, which focuses on drop stretching and breakup in a steady flow. Finally, in the third section we examine the interfacial-tension-driven motion of an elongated drop in a quiescent fluid, including a short description of the influence of surfactant on the growth of capillary waves.

Following I, the deformation is presented as a function of C^*, where $C^*=C/(1-\beta)$. Thus, the effects of the mean decrease in interfacial tension that occurs due to the presence of uniformly distributed surfactant at concentration Γ_0 is built into the nondimensionalization. The effect of surfactant described here is due solely to nonuniform distributions of surfactant along the interface and to the dilution of surfactant as the drop deforms and its total interfacial area increases.

A. Steady drop deformation as a function of viscosity ratio

The steady shapes of viscous drops in an extensional flow are ellipsoidal and can be characterized by either of two parameters: D_f or L/a, where $D_f=(L-B)/(L+B)$, L is the half-length of the drop, and B is the half-breadth of the drop. The deformation of the drop increases with the capillary number up to a limit point (the critical capillary number) above which there are no steady drop shapes (the drop stretches and "breaks up").

The effect of viscosity ratio on the deformation of a surfactant-free drop is well established (see, for example, Ref. 16). For moderate to high viscosity ratios ($\lambda>0.5$), the deformation of the drop is largely insensitive to the viscosity ratio and, the critical capillary number and critical deformation (the largest steady deformation of the drop) are also, approximately, independent of λ. For $\lambda<0.5$, on the other hand, the critical capillary number and the critical deformation increase significantly with decreases in λ. Here, we examine the influence of λ in the presence of surfactant.

It is expected that the influence of surfactant on the drop deformation will be diminished as the viscosity ratio increases. Indeed, this expectation is confirmed by the results in Fig. 2, which show the deformation as a function of the capillary number for $\beta=0.5$ with $\gamma=0.1$, for $\beta=0.3$ with $\gamma=1000$, and for uniform surfactant coverage, i.e., $\beta=0$, at each of three viscosity ratios: $\lambda=0.1$, 1.0, and 10.0. In each figure we see that for $\beta=0.3$, $\gamma=1000$ (convection dominated surfactant mass transfer), the deformation for a given capillary number is increased relative to the case of uniform surfactant coverage. On the other hand, for $\beta=0.5$, $\gamma=0.1$ (diffusion dominated) the deformation is

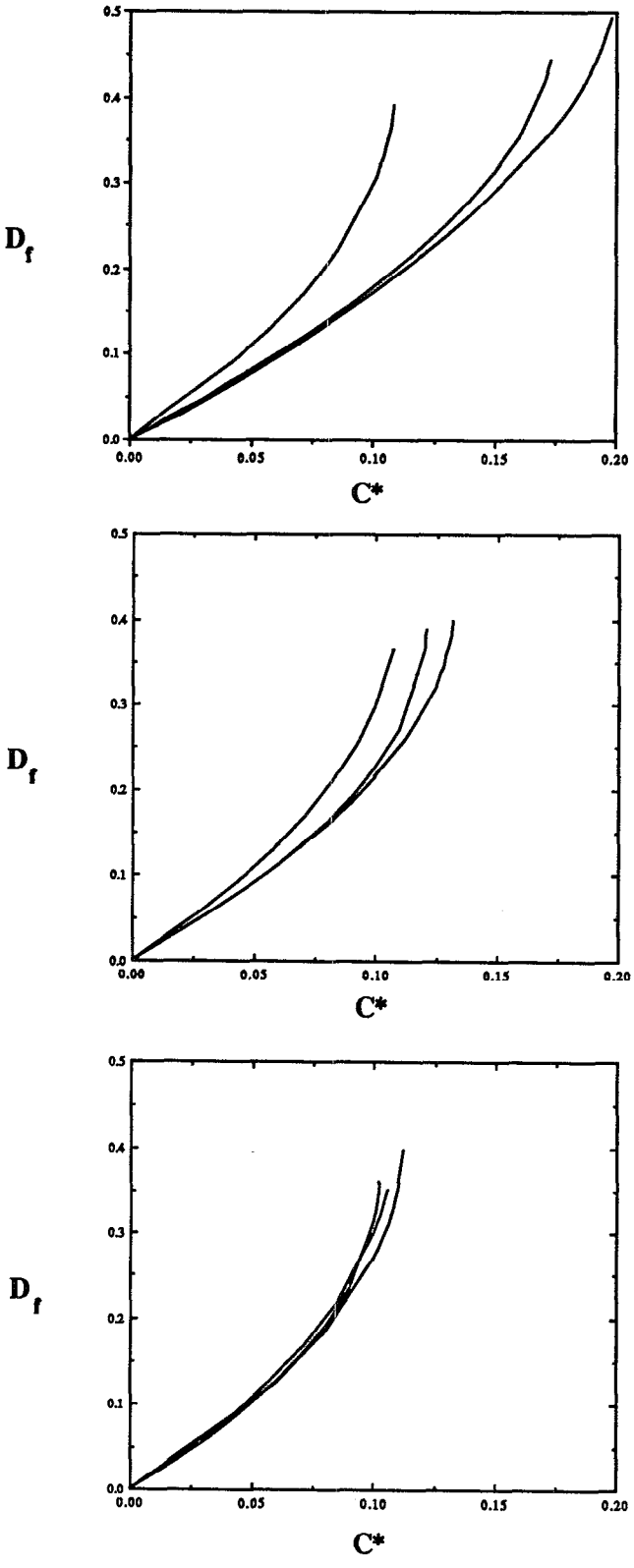

FIG. 2. The effect of surfactant on the deformation of drops at different viscosity ratios. The top figure is for $\lambda=0.1$; the middle figure is for $\lambda=1.0$; and the bottom figure is for $\lambda=10.0$. The rightmost curves are for $\beta=0.5$ and $\gamma=0.1$; the leftmost curves are for $\beta=0.3$ and $\gamma=1000$; the center curves are for a uniform, unchanging concentration of surfactant.

decreased. However, in both cases, the effect of surfactant decreases sharply with increasing viscosity ratio.

For large values of γ, there are substantial gradients in interfacial tension on the interface. These gradients lead to Marangoni stresses that retard the motion of the drop interface and the drop behaves as though it is more viscous. In the absence of surfactant, high viscosity ratio drops are deformed to a greater extent than low viscosity ratio drops at the same capillary number due to the enhanced action of tangential stresses along the drop interface. For the same reason, one might have expected drops with large surfactant gradients to be more deformed than drops of the same viscosity without surfactant gradients, and this is indeed what is observed. However, it should also be noted that increased concentrations of surfactant at the end of the drop require an increase in curvature, and this may also contribute to the increased deformation.

For small values of γ the surfactant concentration is nearly uniform; the effects of Marangoni stresses are minimal. However, since the *amount* of surfactant on the interface is fixed in these simulations, the average concentration of surfactant decreases as the drop deforms. This increases the interfacial tension and decreases the deformation relative to a drop that has a fixed *concentration* of surfactant ($\beta=0$).

As the viscosity ratio is increased, these two surfactant effects are masked. The interface of the drop is already substantially retarded (relative to $\lambda=1$) by the high viscosity of the drop fluid when $\lambda=10.0$, so that a decrease in interfacial velocity due to Marangoni stresses is only incremental and there is little change in the deformation. The effect of dilution is also masked at high viscosity ratios because the maximum degree of steady deformation is limited and breakup thus occurs before significant dilution is realized.

In Fig. 3, we examine the effect of viscosity ratio for fixed values of β and γ: $\beta=0.5$, $\gamma=0.1$ and $\beta=0.3$, $\gamma=1000$. In the former case, the deformation at fixed C^* decreases with decreasing viscosity ratio, analogous to the change in deformation that occurs for a surfactant-free drop. In the latter case, the data for different viscosity ratios are virtually indistinguishable (the line marked "linear" in Fig. 3 is thicker because it is actually three nearly overlapping lines).

The results in Fig. 3 are analogs to those in Fig. 2. For large values of γ, the interfacial velocity is substantially retarded by the Marangoni stresses. The effect of viscosity ratio on interfacial velocity is, therefore, incremental and the effect on the deformation is small. For small values of γ, the Marangoni stresses are minimal. Consequently, changes in the viscosity ratio effect the interfacial velocity and alter the deformation in much the same way as for a surfactant-free drop.

The linear equation of state [Eq. (2)] was used for the results discussed above. The nonlinear equation of state [Eq. (3)] increases the deformation for equivalent values of β and γ because it reduces the interfacial tension to a greater extent in regions of high surfactant concentration. However, it does not qualitatively alter the role of viscosity

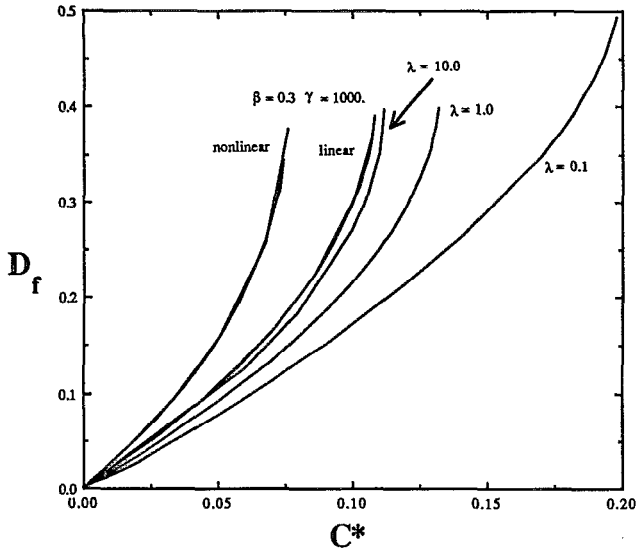

FIG. 3. The effect of viscosity ratio changes at different surfactant conditions. The three curves specified by their viscosity ratio have $\beta=0.5$ and $\gamma=0.1$. For $\beta=0.3$ and $\gamma=1000$, there are five curves plotted that appear as though they were two. For the linear surfactant, equation of state results are plotted for $\lambda=0.1$, 1.0, and 10.0, however, they are virtually indistinguishable. For the nonlinear equation of state the results are plotted for $\lambda=0.1$, 1.0. (Note that the two leftmost curves in the figure are thicker than the others because the separate simulations are not exactly coincident.)

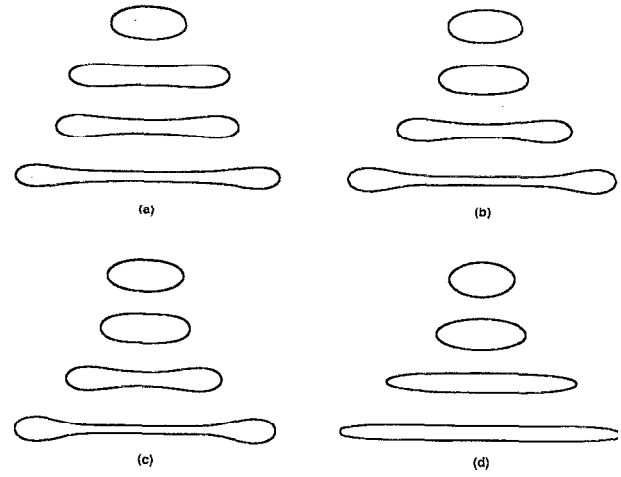

FIG. 4. A comparison of the shapes of stretching drops for a viscosity ratio of unity. Series (a) is for a surfactant-free drop. The dimensionless times are, reading downward, $t=0$, $t=321.6$, $t=326.4$, and $t=331.2$; series (b) is for $\beta=0.5$ and $\gamma=0.1$, $t=0$, $t=170.4$, $t=230.4$, and $t=244.8$; series (c) is for $\beta=0.5$ and $\gamma=10.0$, $t=0$, $t=265.1$, $t=351.5$, and $t=363.5$; and series (d) is for $\beta=0.5$ and $\gamma=1000$, $t=0$, $t=98.9$, $t=197.3$, and $t=209.3$. For each experiment, the difference between the capillary number and the critical capillary number is slightly different. This causes the differences in the elapsed times prior to stretching. An analysis of the stretching *after* this initial period shows that, for all conditions examined in this study, the rate at which the drop stretches approaches that of a line element of the fluid.

ratio on the deformation of a drop with surfactant. This is also shown in Fig. 3. For $\beta=0.3$, $\gamma=1000$, and $\Gamma_\infty=5.0$ there is virtually no effect of viscosity ratio on the deformation, as with the linear equation of state. The only difference due to the nonlinear equation of state is that the steady deformation is shifted to smaller capillary numbers because of a larger decrease in the average interfacial tension.

B. Transient drop extension

When the capillary number is increased beyond the critical capillary number, there is no steady drop shape. At this point the drop stretches, and depending on the drop properties and the surfactant conditions, the drop may fragment. In this section we examine the influence of surfactant on drop stretching and breakup. The initial conditions for these simulations are that the drop is deformed to its critical deformation, and then the capillary number is increased incrementally.

Newtonian drops without surfactant are known to display two general modes of transient motion.[2,17,18] A drop of intermediate to large viscosity ratio ($\lambda>0.5$) initially stretches into a cigarlike shape that continues to increase in aspect ratio until the midsection of the drop forms a waist. The waist then thins as the drop stretches further and the ends of the drop appear bulbous. On the other hand, drops of low viscosity ratio ($\lambda<0.5$) initially form a spindle shape. This shape is retained as further stretching occurs, and bulbous ends do not typically form. After an incipient period, drops of all viscosity ratios stretch at a rate commensurate with a line element of the fluid and can be stretched to large aspect ratios ($L/a>20$) without fragmentation (also see Ref. 19).

In Fig. 4, we present the shapes of stretching drops for $\beta=0.5$ at three different values of γ, and for a surfactant-free drop. In the latter case [Fig. 4(a)], the numerical simulation reproduces the shape evolution described above. Surfactant has two effects on the shape of a stretching drop: one due to large localized surfactant concentrations and one due to surfactant gradients. The first effect is more obvious and occurs for $\gamma=1000$ [Fig. 4(d)]; this drop never develops bulbous ends as it stretches, due to the high surfactant concentrations and low surface tension in this region. For $\gamma=0.1$ and 10.0 the shape of the drop is also changed by the surfactant, albeit in a more subtle way. The waists of these drops are smaller in diameter than that of a drop without surfactant, and are thinning more quickly. Overall, the shape of the stretching drops is determined by the degree to which the surfactant alters the balance between normal and tangential stresses on the drop interface.

Normal stresses alone act to deform a surfactant-free drop into a spindle shape.[20] This is the case for very low viscosity ratios, where the drop phase cannot support tangential stresses. At larger viscosity ratios, tangential stresses act along the interface from the midpoint of the drop toward the ends and cause the drop to form a waist as it stretches. Surfactant accumulates along those regions of the interface where the flow converges, lowers the local interfacial tension, and thus requires a higher degree of curvature in order to maintain the normal stress boundary condition. In uniaxial extension, these regions occur at the

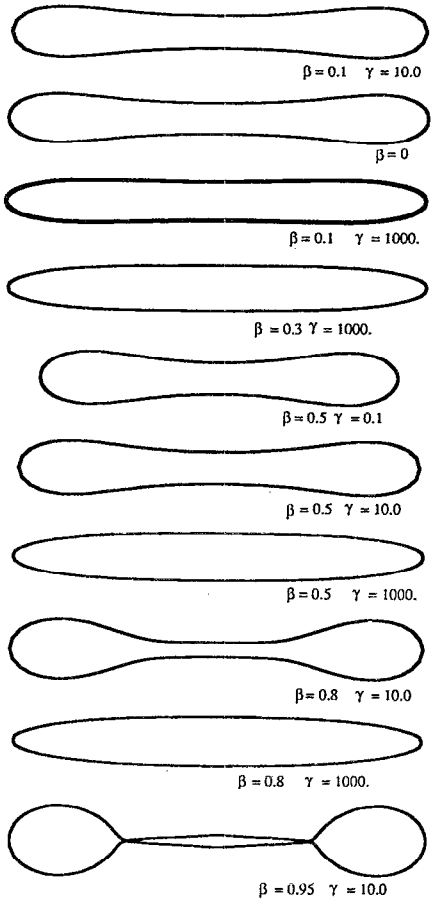

FIG. 5. A comparison of the shapes of stretching drops at an aspect ratio of approximately $L/a=4$ for $\lambda=1.0$.

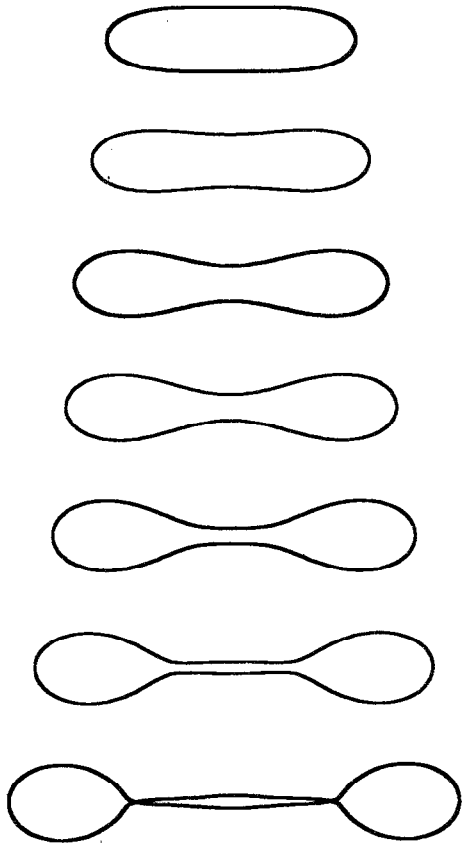

FIG. 6. The stretching of a drop with $\beta=0.95$, $\gamma=10.0$, and $\lambda=1.0$. The simulation is stopped when pinching occurs in the last drawing. The dimensionless times are, reading downward, $t=0$, $t=1201.6$, $t=1265.4$, $t=1289.6$, $t=1305.6$, $t=1313.5$, and $t=1321.5$.

ends of the drop and preclude the formation of bulbous ends for large γ. However, as discussed in the previous section, *gradients* in surfactant concentration also retard the interfacial velocity and cause the drop to appear as though it was more viscous. In this manner, surfactant *gradients* augment the formation of bulbous ends and increase the rate of thinning of the waist, and it is this effect that is evident at $\gamma=0.1$ and 10.

We compare the effects of surfactant on the transient shapes of ten drops in Fig. 5. The viscosity ratio for each of these drops is unity. The shapes shown are an instantaneous "snapshot" for an aspect ratio (L/a) of approximately 4. The drops have ellipsoidal or cigarlike shapes without bulbous ends when $\gamma=1000$ and, as expected, this tendency is enhanced with increasing β (i.e., as the surface tension becomes increasingly sensitive to Γ). For these drops, the interfacial tension at the ends of the drop is substantially reduced, and this prevents the formation of bulbous ends. There is no suppression of the bulbous ends when γ is smaller. Rather, the waists of these drops decrease in diameter as β increases, making the bulbous ends appear more prominent. As β increases with γ fixed, larger gradients in the interfacial tension are present, and thus the interface is further retarded. Evidently, this leads to thinning of the waist.

In the last drawing in Fig. 5, the waist of the drop has decreased in diameter to the point at which it is ready to fragment or "pinch off." In Fig. 6 the time evolution of the shape of this drop is shown. The figure begins with the drop at its critical deformation. When the capillary number is increased, the drop stretches slowly at first and transforms from an ellipsoidal shape to one with a waist and bulbous ends. As time elapses, the waist thins at an increasing rate until it is about to pinch off when the simulation is terminated.

Previous studies, both experimental and theoretical, have shown that Newtonian drops with no surfactant do *not* fragment while stretching for aspect ratios (L/a) at least up to ten.[16] For much larger aspect ratios ($L/a>25$), Rumscheidt and Mason[21] report that stretching drops may fragment due to the growth of capillary waves. Fragmentation of drops by a deterministic, hydrodynamic mechanism, as demonstrated in Fig. 6, has not previously been observed in steady flows. As shown in Fig. 7, the simulations predict that this flow-induced fragmentation occurs for drops with $\lambda=1$ for $\beta\geqslant 0.5$ and $\gamma<100$. Not surprisingly, the aspect ratio necessary to induce pinching decreases with increasing β. For smaller values of β and larger values of γ, drops can be stretched to large aspect ratios ($L/a>15$) without pinching. Pinching is not excluded from further evolution of the shape, however, the

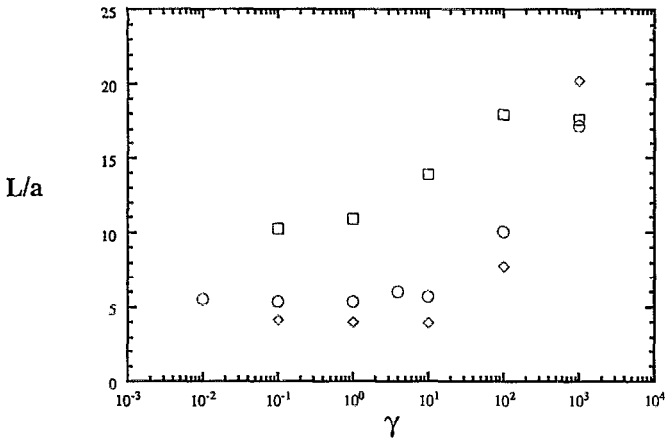

FIG. 7. The aspect ratio (L/a) to which drops can be stretched in steady extensional flow prior to fragmentation by "pinching." The diamonds ($\diamond$) are for $\beta=0.95$; the circles ($\circ$) are for $\beta=0.8$; and the squares ($\square$) are for $\beta=0.5$. The lengths necessary to fragment drops with smaller values of β are greater than 15. The accuracy in the aspect ratio at fragmentation for aspect ratios greater than 15 (in this figure for $\gamma=1000.0$) is uncertain (though clearly greater than 15) due to an insufficient number of collocation points being used to resolve the drop shape.

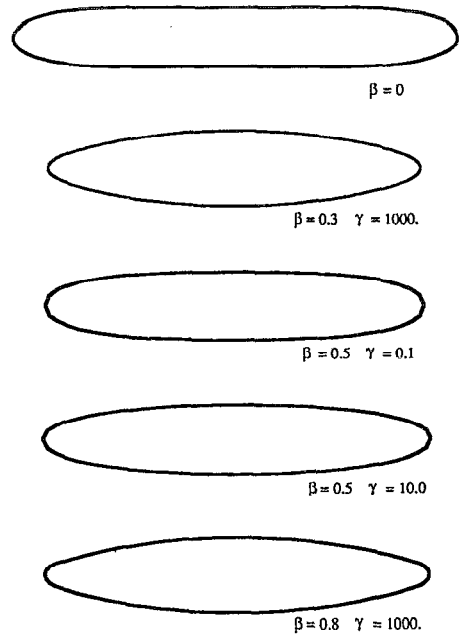

FIG. 8. A comparison of the shapes of stretching drops at an aspect ratio of approximately $L/a=3$ for $\lambda=0.1$.

large number of collocation points required to resolve the shape renders the simulation computationally prohibitive.

The influence of surfactant on the shape of a stretching drop decreases with increasing viscosity ratios. For $\lambda>1$, larger values of γ are needed to suppress the formation of bulbous ends. Since tangential stresses are more important in determining the shapes of higher viscosity drops and since the interfacial velocity decreases with increasing λ, the surfactant concentrations at the end of more viscous drops are smaller for a given value of γ.

For $\lambda<1$, surfactants have a more prominent role in determining the drop shape, since large concentrations of surfactant accentuate the tendency of the drop to form a spindle shape. In Fig. 8, we compare the transient shapes of five different drops with a viscosity ratio of 0.1; the aspect ratio (L/a) of these drops is approximately 3. For $\gamma=1000$, the drop shapes are notably more spindle in character; the ends of the drop are more highly curved and less rounded.

The interfacial velocity of a drop increases with decreasing viscosity ratio. This leads to larger surfactant concentrations at the ends of low viscosity drops for the same values of β and γ. In our simulations, the concentration often reaches the level where the interfacial tension is decreased to *zero* for low viscosity drops. When this occurs the drop shape becomes pointed at the end (a permissible shape in the absence of interfacial tension) and appears to stretch quickly. The pointed shapes in our simulations resemble shapes observed just prior to tip streaming.[21,22] Unfortunately, the simulation cannot resolve further evolution of the shape due to the (near) singularity in curvature associated with a (nearly) pointed end. Consequently, the simulations are unable to determine, definitively, if tip streaming subsequently occurs.

Tip streaming has been observed in the deformation of both Newtonian drops[21] and a wide variety of polymeric drops.[22] In a recent thesis, de Bruijn[23] has demonstrated experimentally that the presence of surfactants may lead to tip streaming. In his experiments, the small droplets ejected from the ends were collected and their interfacial tension was less than the original drop. The obvious interpretation to attach to this description is that surfactant, present in the solution, is adsorbed on the interface and is swept to the ends leading to tip streaming though the exact mechanism for the formation of these small drops remains unknown.

In an earlier paper,[22] we observed that tip streaming occurs for polymeric drops under a number of different conditions. For viscosity ratios greater than unity, the onset or existence of tip streaming appeared to depend on the Deborah number (the ratio of the time scale of the flow to the relaxation time of the fluid). For Deborah numbers greater than order unity, tip streaming occurred in association with overall stretching of the drop, whereas it did not occur at all for small Deborah numbers. For small viscosity ratios, tip streaming occurred for all polymeric drops examined, even those having only a few hundred ppm of polymer dissolved in solution, but stretching of the drop did not occur. Since the viscoelastic stresses in a polymeric drop would be expected to inhibit the formation of highly curved or pointed ends, a satisfactory explanation of these results was not offered in our original publication. However, the present simulations are suggestive of a better explanation.

The polymers used in the viscoelastic drop experiments were water soluble, organic polymers. Thus, they contain chemical structures that are soluble in water, but also some parts that would be soluble in an organic solvent. This suggests that the polymers might exhibit some tendency to

accumulate at the interface between the water and the organic suspending fluid. Indeed, measurements of the equilibrium interfacial tensions between the polymer solutions and the continuous phase fluid show small, but significant, reductions compared to the values with pure water, and this provides a further indication that the polymers may have been acting as surfactants. In this case, the contribution of the polymer to drop deformation would represent a sum of its effects via changes in the bulk rheological properties and via its action as a surfactant. In the latter case, the high molecular weight of the polymer would imply a low surface diffusivity and thus high surface Péclet numbers, leading to high concentrations at the ends of the drop. The present numerical simulations show that, particularly for low viscosity ratios, this would lead to the formation of highly curved or pointed ends and possibly tip streaming. Our speculation is that the effects of the polymer acting as surfactant are dominant for water soluble polymers considered over any bulk rheological effect. This speculation is supported, to some degree, by the experimental observation that shapes with pointed ends and tip streaming were obtained for a wide variety of different polymer solutions, in spite of the fact that these solutions exhibit a broad range of bulk rheological properties.

C. The motion of an extended drop in an otherwise quiescent fluid

The second group of unsteady motions considered is that of a previously stretched drop in an otherwise quiescent fluid. This motion occurs when a drop is stretched by a flow that is stopped or from which the drop is removed. The initial shape, the viscosity ratio, and the surfactant distribution determines the subsequent motion of the drop. Here, we only consider the case $\lambda=1$.

The motion of a deformed, surfactant-free drop is also well established (see, for example, Refs. 2, 17, and 18). Moderately deformed drops revert to a spherical shape while highly deformed drops fragment by "end pinching," a deterministic, interfacial-tension-driven motion. End pinching does not depend on the *fine* detail of the initial shape, and is entirely different from capillary wave breakup. Generally, drops do not fragment as a consequence of a capillary wave instability, unless they are stretched to very large aspect ratios ($L/a>10$).

Surfactants *directly* influence the retraction of a drop by altering the interfacial tension distribution. Nonuniform distributions directly affect the shape evolution in two ways. First, at the ends of the drop the interfacial tension is lower than in the midsection, owing to the higher concentration of surfactant there. Second, Marangoni stresses that arise due to gradients in surfactant concentration augment the interfacial flow and enhance the retraction of the drop. The surfactant redistributes on the interface as the drop retracts due to diffusion and the tangential motion of the interface. However, our simulations show that the time scale for this redistribution is much slower than that for changes in shape.

Surfactants also influence the retraction of a drop *indirectly* by altering the initial shape. In the present simulations, the initial shapes and concentration profiles are taken from simulations of stretching drops. Surfactant effects, such as the suppression of bulbous ends, emerge in these simulations as initial conditions. As we shall show, this indirect effect is more influential in determining the subsequent motion of the drop than the direct effects.

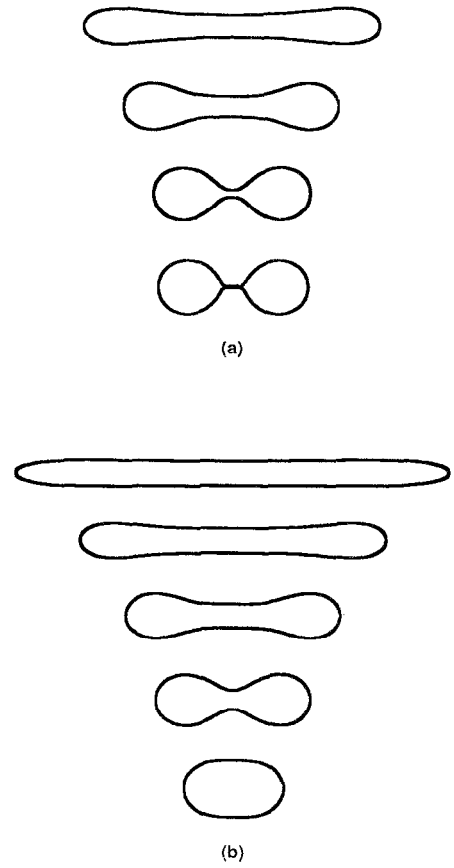

FIG. 9. Retraction of drops in a quiescent fluid. Part (a) is for a drop without surfactant; reading downward, $t=0$, $t=7.2$, $t=16.8$, and $t=19.2$. Part (b) is for a drop with an initial surfactant distribution $\beta=0.3$, $\gamma=1000$; reading downward, $t=0$, $t=12.0$, $t=24.0$, $t=36.0$, and $t=48.0$. The surfactant distribution is determined from simulations of the stretching drops and both drops have a viscosity ratio of unity.

In Fig. 9 we compare the motion of two drops: one surfactant-free (a) and one with surfactant (b) [$\beta=0.3$ and $\gamma=1000$]. The drop in Fig. 9(a) fragments into two daughter drops and a satellite droplet as a result of end pinching. The initial aspect ratio of this drop is, approximately, the smallest aspect ratio that results in end pinching. The drop with surfactant, (b), does not fragment, although it has a *greater* initial aspect ratio. This is one of the most significant effects of surfactant on the surface-tension-driven motion of elongated drops: larger extensions of the drop are permissible without producing end pinching.

The smallest elongation of a drop that results in breakup by end pinching is plotted in Fig. 10. For values of $\gamma\leqslant 10$, the minimum aspect ratio remains approximately constant, although there is some decrease with increasing β. For large values of γ, the critical aspect ratio increases

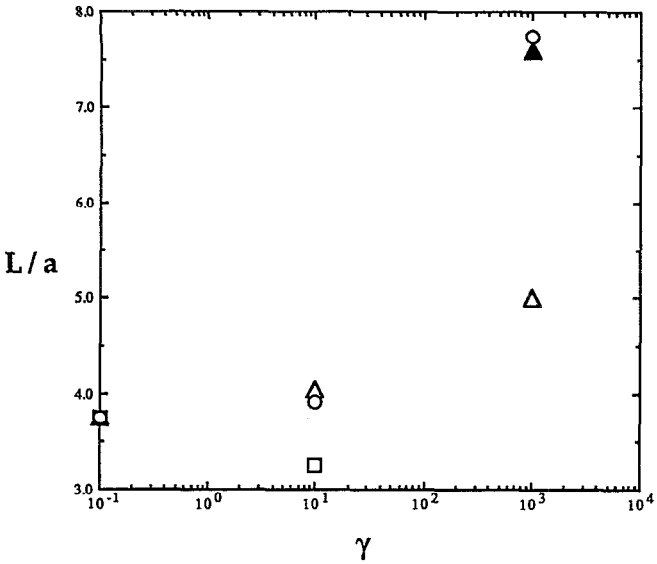

FIG. 10. A plot showing the deformation needed to induce end pinching on a drop in a quiescent fluid. The open triangles (△) are for $\beta=0.1$, the solid triangles (▲) are for $\beta=0.3$, the circles (○) are for $\beta=0.5$, and the squares (□) are for $\beta=0.8$. Note that at $\gamma=0.1$, there are three overlapping points.

significantly, thus making the drop more difficult to break, and the effect becomes more pronounced as β increases. Both of these effects are the result of changes in the initial drop shape. Drops that form thin waists as they stretch are more easily fragmented by end pinching (note the point $\beta=0.8$, $\gamma=10$, open square). On the other hand, drops with large values of γ do not form bulbous ends as they stretch. During retraction, the ends of these drops must become bulbous prior to end pinching. The retraction that occurs while the ends of the drop are becoming bulbous allows the drop to return to a spherical shape. To demonstrate that this effect is due to changes in the initial shape and not the surfactant concentration gradient, we present a slightly contrived simulation in Fig. 11.

The drop in Fig. 11(a) has the same initial shape as the surfactant laden drop in Fig. 9. That is, the initial shape of this drop was generated by the stretching of a drop with surfactant ($\beta=0.3$ and $\gamma=1000$), but the surfactant gradient was "removed" prior to retraction. In Fig. 9, we saw that a surfactant-free drop with a *smaller* aspect ratio undergoes end pinching. Here, the drop does not fragment, and the results are similar to those for the surfactant laden drop in Fig. 9.

The drop in Fig. 11(b) has an initial shape that is generated by the stretching of a surfactant-free drop (the same initial shape as the surfactant free drop in Fig. 9). We have artificially added a distribution of surfactant to the drop corresponding to $\beta=0.3$ and $\gamma=1000$ (that is, we applied the distribution of surfactant from a drop with the same elongation that had been stretched under the conditions $\beta=0.3$ and $\gamma=1000$). This drop fragments, whereas the surfactant-laden drop in Fig. 9 did not, although it had a greater initial aspect ratio. The results in Fig. 11 clearly show the dominant influence of initial shape in drop retraction and end pinching. Note that in both Figs. 9 and 11 the surfactant-laden drops retract more slowly, due to the decrease of the interfacial tension caused by the surfactant.

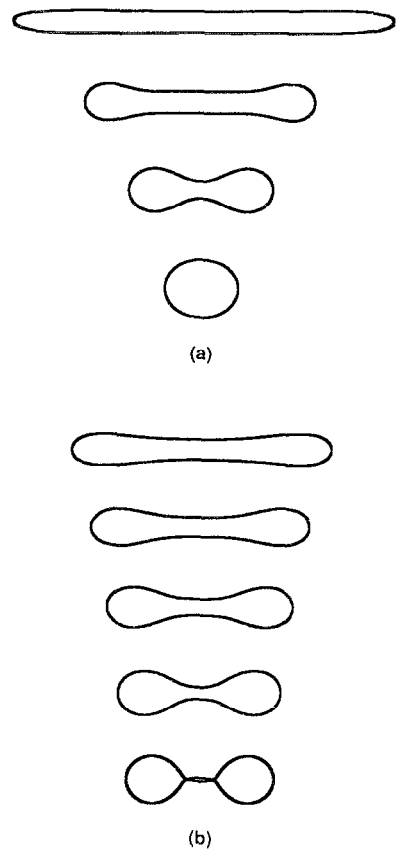

FIG. 11. This figure shows the dependence of retraction on the initial drop shape. The initial shapes of this figure have been exchanged from that in Fig. 9. In this figure, the drop on the top has no surfactant effects, but its initial shape is taken from the stretching of a drop with a surfactant distribution of $\beta=0.3$, $\gamma=1000$; reading downward, $t=0$, $t=12.0$, $t=24.0$, and $t=36.0$. The drop on the bottom has a surfactant distribution corresponding to $\beta=0.3$, $\gamma=1000$, but this figure takes its shape from the stretching of a surfactant-free drop; reading downward, $t=0$, $t=6.0$, $t=12.0$, $t=18.0$, and $t=25.0$.

Drops must be stretched to initial aspect ratios that are greater than those in Figs. 9 and 11 to permit observable capillary wave growth. Furthermore, capillary waves were not observed on the interface in any of the simulations while the drops were stretching. This latter result is in accord with theory[24] and experiment.[18] In the absence of surfactant, capillary waves grow along the midsection of a highly deformed drop in a quiescent fluid and cause it to fragment into several equally sized and spaced droplets while end pinching simultaneously causes fragmentation at the ends of the drop.

At low Reynolds number, the linear stability theory for capillary waves on a surfactant-free cylindrical thread dictates that interfacial tension only sets the time scale. The wavelength having the maximum growth rate depends upon the viscosity ratio, but not the interfacial tension. On the other hand, the exponential growth rate of the capillary waves is linearly dependent on interfacial tension. Consequently, by reducing the interfacial tension, we expect sur-

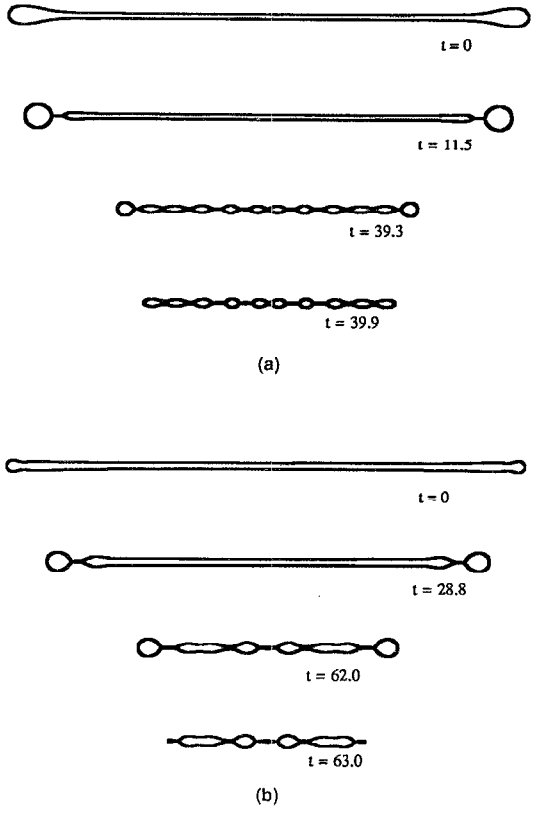

FIG. 12. Capillary wave growth on an extended drop. Part (a) is for a drop without surfactant. Part (b) is for a drop with a surfactant distribution developed during stretching: $\beta=0.3$ and $\gamma=1000$.

factants to alter the time scale for capillary wave growth. Near the end of the drop where the surfactant concentration is high, the capillary growth rate is slow. In the middle of the drop where the concentration is low the growth rate is larger.

Several previous researchers have considered the effect of surfactants on capillary wave growth (for example, Refs. 25–27). However, these studies have focused on the roles of the interfacial viscosity and elasticity caused by the adsorbed surfactant. In our simulations it is assumed that the interface is completely described by the interfacial tension, which varies with surfactant concentration.

An example of the effect of surfactant on the growth of capillary waves is shown in Fig. 12. In this figure we compare two drops with approximately the same initial elongation: the drop in Fig. 12(a) is surfactant-free, while the drop in Fig. 12(b) has $\beta=0.3$ and $\gamma=1000$. The initial conditions for both drops were taken from simulations of stretching drops. In order to generate this figure, we have assumed that "pinch-off" occurs when the interfacial separation at any axial location becomes too small to be resolved numerically (generally less than 10^{-3}). The portion of the drop on the outside of that axial position is subsequently discarded by the numerical routine and the point of minimum interface separation becomes the new end of the drop. The half-drops in this figure are represented by 90 collocation points; after "pinch-off" (where some points are lost) the points representing the remainder of the drop are respaced and increased in number back to 90. There is no initial capillary wave perturbation superimposed on the drop interface.

In Fig. 12(a) (a surfactant-free drop) end pinching occurs twice, at $t=11.5$ and 39.3, before capillary waves cause fragmentation of the remaining thread. Breakup due to capillary wave growth is accompanied by the formation of ten (approximately) equally sized drops. Satellite droplets form between the drops, although their subsequent dynamics requires additional, careful numerical simulation.[28] The wavelength of the fastest growing mode is approximately 9.3 times the initial radius of the cylindrical midsection of the drop. This is in fair agreement with the fastest growing linear mode from theory (10.5).

In Fig. 12(b) the growth of capillary waves on a drop with a large initial interfacial tension gradient is shown. End pinching occurs for this drop, but it requires a longer elapsed time due to the lack of bulbous ends in the initial shape. Capillary waves are evident along the midsection of the drop at $t=62.0$ when end pinching occurs for the second time. Rather than several equally sized and spaced drops, two drops are formed in the middle with a satellite drop between. Two larger drops are formed near the end of the drop. In addition to the obvious qualitative change in the shape of this drop as it fragments, note, also, that a significantly longer time was required prior to the appearance of the capillary waves.

The influence of surfactants is clearly evident in Fig. 12. The growth rate for the capillary waves is slowed and there is a distribution of growth rates over the length of the drop. Capillary waves form fastest in the middle. At the same time, the waist of the drop grows as it retracts. Thus the drops in the middle are the smallest, since they occur when the waist of the drop is smallest. Capillary drops that form later and farther from the center are larger in diameter.

IV. SUMMARY

In this study, we generalize the results of Stone and Leal[9] on the effects of insoluble surfactant on the deformation of viscous drops. We find that for large γ (large Péclet numbers; convection dominated motion of the surfactant on the interface), the *steady* drop shapes are deformed more in the presence of surfactant than when the interface has a constant interfacial tension. For small γ (small Péclet numbers), dilution causes a decrease in the deformation. These effects become more prominent as the viscosity ratio decreases and are essentially masked for $\lambda \geqslant 10.0$. For essentially identical reasons, the effect of changes in the viscosity ratio are masked at large γ.

The effect of surfactants on the *unsteady* motion of a drop also results from the combined effects of surfactant accumulation at the ends and dilution. These effects are best understood by considering their influence on the normal and tangential stress balances at the interface. In regions of low interfacial tension the shape of the drop becomes more highly curved in order to maintain the normal stress balance. This causes suppression of the bulbous ends

usually seen when a viscous drop is stretched. For small viscosity ratios, large γ (convection dominated motion) leads to drops with spindlelike shapes with pointed ends. These pointed ends most likely lead to tip streaming, like that observed experimentally with some viscoelastic drops, although the simulations are not currently able to resolve this issue. Large surfactant *gradients* retard the interfacial velocity and influence the drop shape predominantly through the tangential stress balance. By retarding the interface, the surfactant gradients cause the drop to behave as though it were more viscous. This leads to thinning of the drop waist, an enhancement of the bulbous ends and, for sufficiently large interfacial tension gradients, leads to fragmentation of the drop.

The motion of elongated drops in a quiescent fluid is most strongly influenced by surfactant through their initial shape. By using the drop shapes that were obtained during simulations of drop stretching, we find that changes in the initial drop shape due to the surfactant have a substantial effect on the retraction process. In particular, the suppression of bulbous ends during stretching inhibits the end pinching breakup of the drop. Surfactants also alter the time scale for capillary wave growth on highly elongated drops and consequently cause the formation of unequal-sized drops from capillary wave breakup. The effects of surfactant on the motion of an elongated drop in a quiescent fluid could substantially alter the drop size distribution in mixing.

ACKNOWLEDGMENTS

This work was supported by grants to LGL and HAS from the Fluid Mechanics Program of the National Science Foundation.

[1]G. I. Taylor, "The viscosity of a fluid containing small droplets of another fluid," Proc. R. Soc. London Ser. A **138**, 41 (1932).
[2]G. I. Taylor, "The formation of emulsions in definable fields of flow," Proc. R. Soc. London Ser. A **146**, 501 (1934).
[3]J. M. Rallison, "The deformation of small viscous drops and bubbles in shear flows," Annu. Rev. Fluid Mech. **16**, 45 (1984).
[4]H. A. Stone, "Dynamics of drop deformation and breakup in time-dependent flows at low Reynolds numbers," Ph.D. thesis, California Institute of Technology, 1988.
[5]R. W. Flumerfelt, "Effects of dynamic interfacial properties on the deformation and orientation in shear and extensional flow fields," J. Colloid Interface Sci. **76**, 330 (1980).
[6]H. P. Greenspan, "On the dynamics of cell cleavage," J. Theor. Biol. **65**, 79 (1977).
[7]H. P. Greenspan, "On the deformation of a viscous droplet caused by variable surface tension," Stud. Appl. Math. **57**, 45 (1977).
[8]D. Zinemanas and A. Nir, "On the viscous deformation of biological cells under anisotropic surface tension," J. Fluid Mech. **193**, 217 (1988).
[9]H. A. Stone and L. G. Leal, "The effects of surfactants on drop deformation and breakup," J. Fluid Mech. **220**, 161 (1990).
[10]S. Y. Lin, K. McKeigue, and C. Maldarelli, "Diffusion-controlled surfactant adsorption studied by pendant drop digitization," AIChE J. **36**, 1785 (1990).
[11]R. Aris, *Vectors, Tensors, and the Basic Equations of Fluid Mechanics* (Prentice–Hall, Englewood Cliffs, NJ, 1962).
[12]A. M. Waxman, "Dynamics of a couple-stress fluid membrane," Stud. Appl. Math. **70**, 63 (1984).
[13]H. A. Stone, "A simple derivation of the time-dependent convective-diffusion equation for surfactant transport along a deforming interface," Phys. Fluids A **2**, 111 (1990).
[14]S. H. Lee and L. G. Leal, "The motion of a sphere in the presence of a deformable interface. II. A numerical study of the translation of a sphere normal to an interface," J. Colloid Interface Sci. **87**, 81 (1982).
[15]G. K. Youngren and A. Acrivos, "On the shape of a gas bubble in a viscous extensional flow," J. Fluid Mech. **76**, 433 (1976).
[16]B. J. Bentley and L. G. Leal, "An experimental investigation of drop deformation and breakup in steady two-dimensional linear flows," J. Fluid Mech. **167**, 241 (1986).
[17]H. P. Grace, "Dispersion phenomena in high viscosity immiscible fluid systems and application of static mixers as dispersion devices in such systems," Chem. Eng. Commun. **14**, 113 (1971).
[18]H. A. Stone, B. J. Bentley, and L. G. Leal, "An experimental study of transient effects in the breakup of viscous drops," J. Fluid Mech. **173**, 131 (1986).
[19]M. Tjahjadi and J. M. Ottino, "Stretching and breakup of droplets in chaotic flows," J. Fluid Mech. **232**, 191 (1991).
[20]A. Acrivos and T. S. Lo, "Deformation and breakup of a slender drop in an extensional flow," J. Fluid Mech. **86**, 641 (1978).
[21]F. D. Rumscheidt and S. G. Mason, "Particle motions in sheared suspensions. 12. Deformation and burst of fluid drops in shear and hyperbolic flows," J. Colloid Interface Sci. **16**, 238 (1961).
[22]W. J. Milliken and L. G. Leal, "Deformation and breakup of viscoelastic drops in planar extensional flows," J. Non-Newtonian Fluid Mech. **40**, 355 (1991).
[23]R. A. de Bruijn, "Deformation and breakup of drops in simple shear flow," Ph.D. thesis, Technische Universiteit Eindhoven, 1989.
[24]T. Mikami, R. G. Cox, and S. G. Mason, "Breakup of extending liquid threads," Int. J. Multiphase Flow **2**, 113 (1975).
[25]F. W. Pierson and S. Whitaker, "Studies of the drop weight method for surfactants solutions. I. Mathematical analysis of the adsorption of surfactants at the surface of a growing drop," J. Colloid Interface Sci. **54**, 203 (1976).
[26]F. W. Pierson and S. Whitaker, "Studies of the drop weight method for surfactants solutions. II. Experimental results for water and surfactant solutions," J. Colloid Interface Sci. **54**, 218 (1976).
[27]S. Whitaker, "Studies of the drop-weight method for surfactant solutions. III. Drop stability, the effect of surfactants on the stability of a column of liquid," J. Colloid Interface Sci. **54**, 231 (1976).
[28]M. Tjahjadi, H. A. Stone, and J. M. Ottino, "Satellite and sub-satellite formation in capillary breakup," submitted to J. Fluid Mech.